JOURNAL OF GUIDANCE, CONTROL, AND DYNAMICS
Vol. 21, No. 6, November–December 1998

High-*g* Barrel Roll Maneuvers Against Proportional Navigation from Optimal Control Viewpoint

Fumiaki Imado*
Shinshu University, Nagano 380, Japan
and
Sachio Uehara†
Mitsubishi Heavy Industries, Ltd., Tokyo 100, Japan

Our previous studies showed that the high-*g* barrel roll (HGB) maneuver generally produces very large miss distance against proportional navigation missiles. The performance of this maneuver is discussed from the viewpoint of optimal control. Numerically obtained three-dimensional optimal evasive maneuvers of a fighter against a proportional navigation missile were those of vertical-S type and horizontal-S type, which are two dimensional in nature. It is shown that the HGB is regarded as a kind of approximation of these optimal maneuvers; however, the HGB is easier to implement than the optimal maneuvers, and we may still insist on the practical effectiveness of the HGB.

Nomenclature

$a_{c\max}$	= missile lateral acceleration command limit
a_p, a_y, a_{pc}, a_{yc}	= missile pitch- and yaw-axis lateral accelerations and their command signals
a_t	= aircraft normal acceleration
g	= acceleration of gravity
h	= altitude
L	= lift
MD	= miss distance
m	= mass
N_e	= effective navigation constant
r, r_x, r_y, r_z	= relative range between missile and aircraft and its inertial x, y, and z components, respectively
T	= thrust
t	= time
v	= velocity
v_c	= closing velocity
x, y, z	= inertial coordinates
α	= angle of attack
γ, ψ	= flight-path and azimuth angles, respectively
$\dot{\boldsymbol{\sigma}}$, $\dot{\sigma}_p$, $\dot{\sigma}_y$	= line-of-sight rate vector and its pitch and yaw components, respectively
$\dot{\sigma}_{xI}$, $\dot{\sigma}_{yI}$, $\dot{\sigma}_{zI}$	= inertial x, y, and z components of $\dot{\boldsymbol{\sigma}}$, respectively
τ	= missile time constant
ϕ	= aircraft roll angle
ω	= high-*g* barrel roll rate
$(\dot{})$	= time derivative

Subscripts

c	= control command signal
f	= terminal (final) value
I	= inertial coordinate
m	= missile
max	= maximum value
min	= minimum value
p	= pitch component
t	= aircraft (target)
y	= yaw or y component
0	= initial value

Presented as Paper 96-3839 at the AIAA Guidance, Navigation, and Control Conference, San Diego, CA, July 29–31, 1996; received June 2, 1997; revision received Dec. 30, 1997; accepted for publication May 29, 1998.

*Professor, Department of Mechanical System Engineering, 500 Wakasato Nagano. E-mail: imado@imado1.shinshu-u.ac.jp.
†Advisor, Aircraft and Special Vehicle Headquarters, 2-5-1 Marunouchi Chiyodaku.

I. Introduction

MANY studies have been performed on the optimal evasive maneuver of an aircraft against a proportional navigation guidance (PNG) missile. To obtain the optimal aircraft maneuver, a high-dimensional, nonlinear, two-point boundary value problem must be solved. Because of the difficulty inherent in this problem, most earlier works use very simple aircraft and missile models, and only a few deal with the three-dimensional problems.[1]

The results of earlier two-dimensional studies showed that optimal evasive maneuvers are a split-S type or a vertical-S type.[2,3] Because these maneuvers are two dimensional in nature, the previous results are valid and may be proved to be optimum in the neighboring extremal sense. The high-*g* barrel roll (HGB) maneuver,[4,5] which is well-known to pilots, however, cannot be analyzed by a two-dimensional study because of its essentially three-dimensional nature.[6,7] As the maneuver surely produces a very large miss distance, we are interested in the maneuver from the point of view of its optimality. Unfortunately, because our algorithm lacked the ability to optimize maneuvers, we could not have obtained three-dimensional optimal maneuvers, but the recent improvement of our algorithm has made it possible.

In this paper, the mathematical model for the three-dimensional pursuit–evasion problem of an aircraft against a PNG missile is shown first. Next, some features of the aircraft optimal evasive maneuvers and HGB are explained. Finally, the exact numerical solution for the three-dimensional pursuit–evasion problem is illustrated, and the nonoptimality of the HGB is shown. The relation between the optimal maneuver and the HGB is also discussed.

II. Mathematical Model

Figure 1 shows the symbols of a missile and an aircraft. Point-mass models are used, and constant mass and velocity are assumed for both vehicles. The system equations are

$$\dot{\gamma}_t = (a_t/v_t)\cos\phi - (g/v_t)\cos\gamma_t \tag{1}$$

$$\dot{\psi}_t = \frac{a_t}{v_t\cos\gamma_t}\sin\phi \tag{2}$$

$$\dot{\gamma}_m = a_p/v_m \tag{3}$$

$$\dot{\psi}_m = \frac{a_y}{v_m\cos\gamma_m} \tag{4}$$

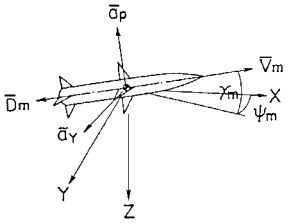

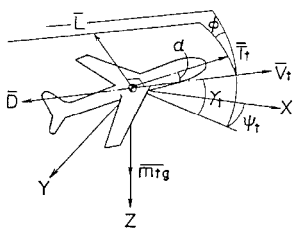

Fig. 1 Missile and aircraft symbols.

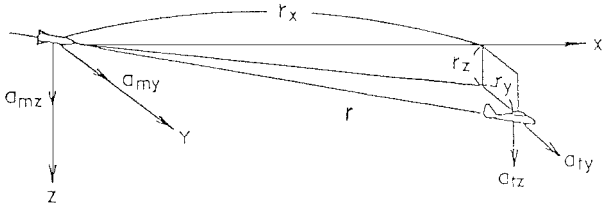

Fig. 2 Relative geometry of vehicles.

$$\dot{r}_x = v_t \cos\gamma_t \cos\psi_t - v_m \cos\gamma_m \cos\psi_m \tag{5}$$

$$\dot{r}_y = v_t \cos\gamma_t \sin\psi_t - v_m \cos\gamma_m \sin\psi_m \tag{6}$$

$$\dot{r}_z = -v_t \sin\gamma_t + v_m \sin\gamma_m \tag{7}$$

$$\dot{a}_p = \frac{a_{pc} - a_p}{\tau} \tag{8}$$

$$\dot{a}_y = \frac{a_{yc} - a_y}{\tau} \tag{9}$$

where $a_t = (L + T_t \sin\alpha)/m_t$ is the aircraft normal acceleration and r_x, r_y, and r_z are relative range components, shown in Fig. 2. In a roll-stabilized PNG missile, pitch and yaw acceleration commands are given by

$$\begin{aligned} a_{pc} &= N_e v_c \dot{\sigma}_p \quad \text{for} \quad |a_{pc}| \le a_{c\max} \\ a_{c\max}\,\text{sign}(a_{pc}) &\quad \text{for} \quad |a_{pc}| > a_{c\max} \end{aligned} \tag{10}$$

$$\begin{aligned} a_{yc} &= N_e v_c \dot{\sigma}_y \quad \text{for} \quad |a_{yc}| \le a_{c\max} \\ a_{c\max}\,\text{sign}(a_{yc}) &\quad \text{for} \quad |a_{yc}| > a_{c\max} \end{aligned} \tag{11}$$

where the missile actual accelerations are approximated through a first-order lag to their commands, as is shown in Eqs. (8) and (9). The line-of-sight rate vector and its components measured in missile pitch and yaw axes are given by

$$\dot{\boldsymbol{\sigma}} = \frac{\boldsymbol{r} \times (\mathrm{d}/\mathrm{d}t)\boldsymbol{r}}{\boldsymbol{r} \cdot \boldsymbol{r}} = \frac{1}{r^2} \begin{bmatrix} r_y \dot{r}_z - r_z \dot{r}_y \\ r_z \dot{r}_x - r_x \dot{r}_z \\ r_x \dot{r}_y - r_y \dot{r}_x \end{bmatrix} = \begin{bmatrix} \dot{\sigma}_{xI} \\ \dot{\sigma}_{yI} \\ \dot{\sigma}_{zI} \end{bmatrix}_I \tag{12}$$

$$\dot{\sigma}_p = -\sin\psi_m \dot{\sigma}_{xI} + \cos\psi_m \dot{\sigma}_{yI} \tag{13}$$

$$\dot{\sigma}_y = \sin\gamma_m (\cos\psi_m \dot{\sigma}_{xI} + \sin\psi_m \dot{\sigma}_{yI}) + \cos\gamma_m \dot{\sigma}_{zI} \tag{14}$$

where v_c is the closing velocity given by

$$v_c = -\dot{r} = \frac{-(r_x \dot{r}_x + r_y \dot{r}_y + r_z \dot{r}_z)}{r} \tag{15}$$

$$r = \left(r_x^2 + r_y^2 + r_z^2\right)^{\frac{1}{2}} \tag{16}$$

For optimal missile avoidance problems, the time histories $a_t(t)$ and $\phi(t)$ must be calculated, which maximize the following final miss distance r_f:

$$J = r_f = r(t_f) \tag{17}$$

where t_f is given from the following closest approach point condition:

$$\Omega \equiv \frac{\mathrm{d}}{\mathrm{d}t}(r^2) = 0 \tag{18}$$

The following constraint is imposed on the aircraft normal acceleration:

$$|a_t| \le a_{t\max} \tag{19}$$

For simplicity, the aircraft control time constants are neglected here. The transformation from the preceding relative coordinates to inertial coordinates is implemented by integrating the following auxiliary equations:

$$\dot{x}_m = v_m \cos\gamma_m \cos\psi_m \tag{20}$$

$$\dot{y}_m = v_m \cos\gamma_m \sin\psi_m \tag{21}$$

$$\dot{z}_m = -v_m \sin\gamma_m \tag{22}$$

$$x_t = x_m + r_x \tag{23}$$

$$y_t = y_m + r_y \tag{24}$$

$$z_t = z_m + r_z \tag{25}$$

III. Performance of HGB and Three-Dimensional Optimal Evasive Maneuver

Table 1 shows some of the parameters employed. Figure 3 shows the initial geometry of the vehicles and symbols. HGB is a maneuver that continuously increases (or decreases) roll angle while simultaneously taking maximum normal acceleration. The feature of the maneuver is well described in Ref. 7; however, for the readers' convenience, it is briefly explained here. A conceptual HGB pattern is shown in Fig. 4. Figure 5 shows the miss distance vs time to go (duration of maneuver until interception) for various aircraft HGB roll rates. In Fig. 5, results are obtained by simulations employing sophisticated realistic aircraft and missile models. The miss distance becomes large and irrelevant to a time-to-go of larger than 3 s if the roll rate $\omega(= \dot{\phi})$ is 1–3 rad/s. On the other hand, in the case of

Table 1 Nominal parameters

Parameter	Value
v_t	300 m/s
$a_{t\max}$	90 m/s^2
v_m	700 m/s
$a_{pc\max}$	300 m/s^2
N_e	4
τ	0.4 s

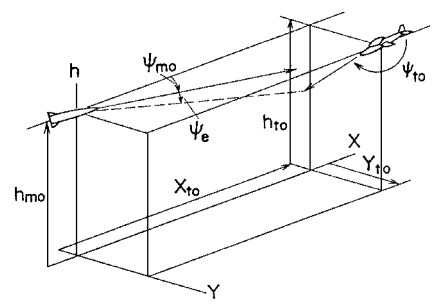

Fig. 3 Initial geometry.

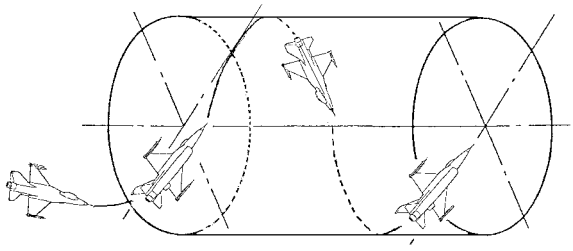

Fig. 4 Typical HGB flight pattern.

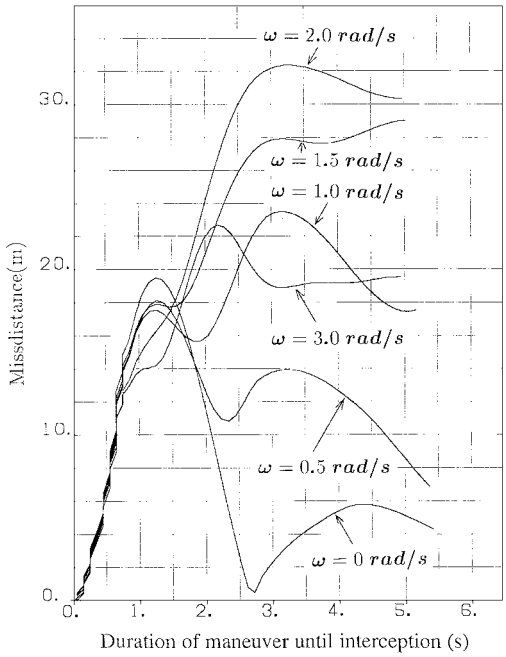

Fig. 5 Effect of duration of maneuver and roll rate.

$\omega = 0$, which corresponds to a split-S type in the two-dimensional maneuver, the miss is relatively small and critically depends on the time-to-go value. In other words, the evasive maneuver has to be started about 1 s before interception in this case. From Fig. 5, it can be said that the HGB is effective if the aircraft takes the maneuver earlier with the proper roll rate.

As the HGB produces very large miss distances, we had the expectation that we might find the optimal solution for missile avoidance in HGBs. To show this, we have tried to solve this optimal control problem by a steepest ascent method.[8,9] The method is a direct method used to solve nonlinear optimal control problems, where a nominal solution is chosen and control variables are iteratively corrected so that the system Hamiltonian becomes maximum. As it is too difficult to solve by employing the same models in Fig. 5, the simplified models shown in Sec. II are employed. The data in Table 1 are chosen to produce almost the same result as the sophisticated models in Fig. 5. As has been noted, the emphasis is placed on the comparison between the optimal evasive maneuver and the HGB; the nominal solution was chosen from that of the HGB. Therefore, if the HGB is optimal, then the controls will be maintained unchanged; however, they have always changed and converged to other types of solutions.

Figures 6–9 show vehicle trajectories and aircraft control histories. Initial missile direction is chosen to lie in the collision course, i.e., $\psi_e = 0$ in Fig. 3, x_{t0} is 3000 m. Figure 6 shows an obtained optimal solution, which clearly shows the feature of the vertical-S pattern, where $\psi_{t0} = 180$ deg. Figures 7 and 8 show two types of neighboring optimal solutions, the features of which correspond to those of the vertical-S and the horizontal-S maneuvers, respectively. In these cases $\psi_{t0} = 165$ deg. This latter solution is obtained through the iterating optimization process, where the initially nominal controls employed are that of the HGB with $\omega = 2$ rad/s, which

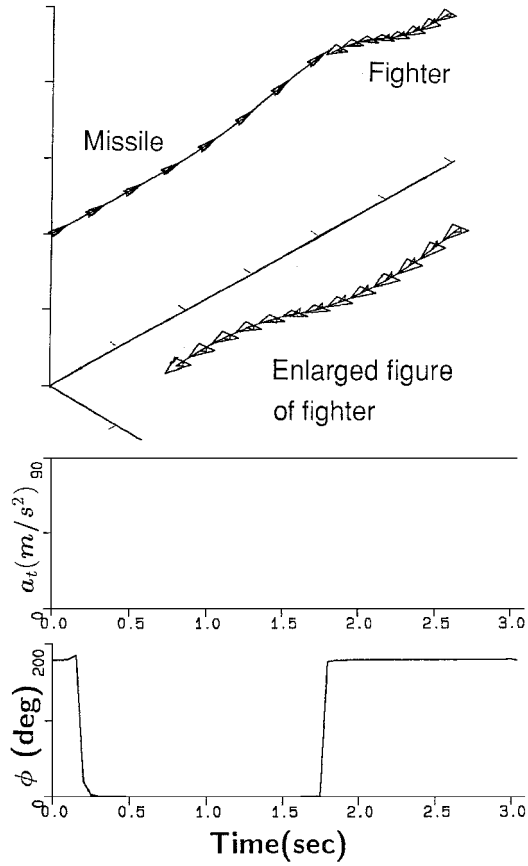

Fig. 6 Vehicle trajectories and control histories ($\psi_{t0} = 180$ deg, vertical-S type).

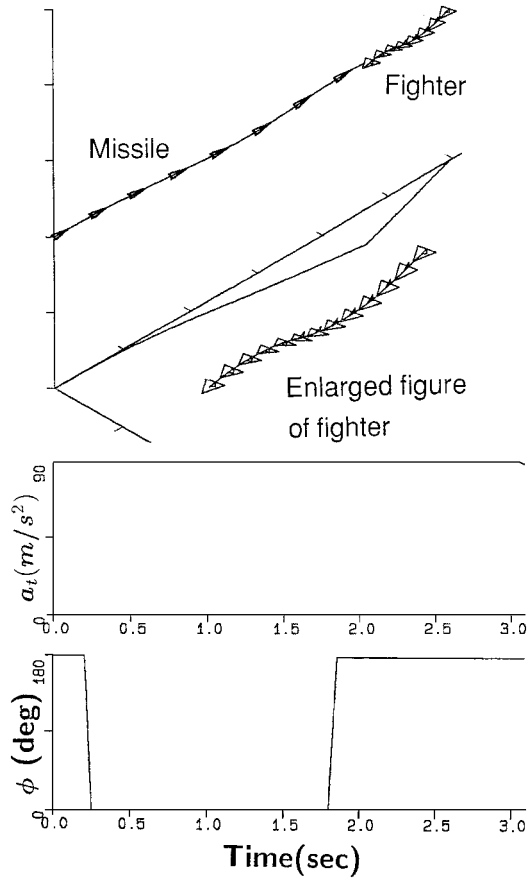

Fig. 7 Vehicle trajectories and control histories ($\psi_{t0} = 165$ deg, vertical-S type).

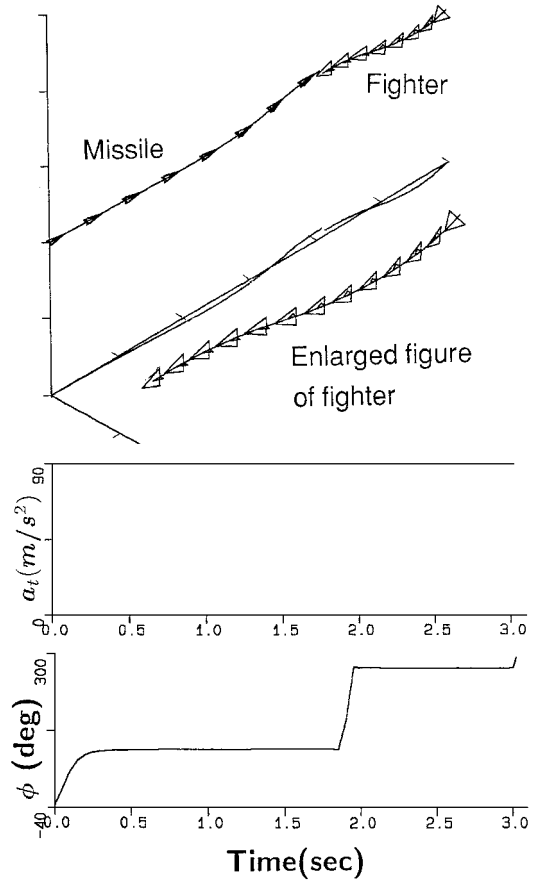

Fig. 8 Vehicle trajectories and control histories (ψ_{t0} = 165 deg, horizontal-S type).

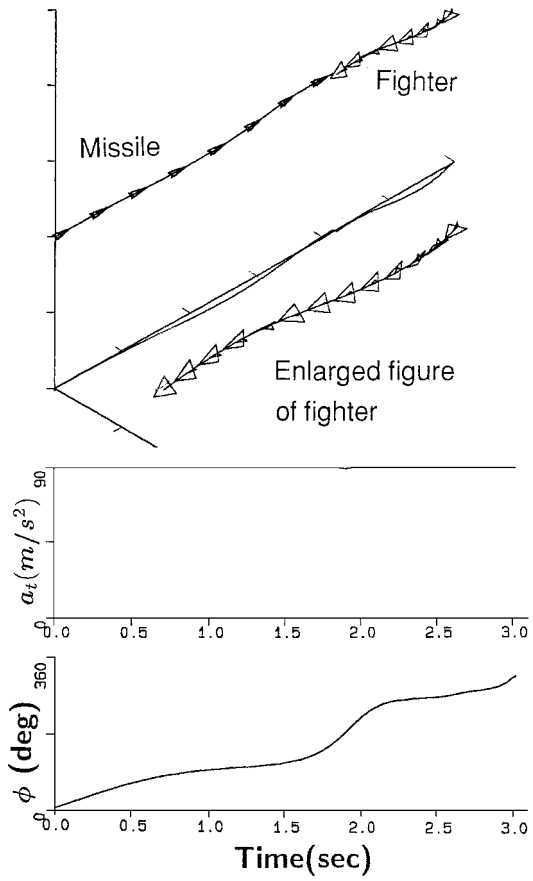

Fig. 9 Example of vehicle trajectories and control histories at an intermediate iteration process.

produces the miss distance (MD) 19.4 m. In the converged maneuver (Fig. 8), MD is 27.7 m, which is surely larger than that of the HGB. Figure 9 shows an intermediate process in the early stage of iteration, where the solution is not at all converged; however, MD is 25.7 m, which is fairly close to that of the converged solution. From the preceding results, we may say that although the HGB is not an optimal maneuver, it is nevertheless easier to implement than an optimal maneuver (because it is very difficult for a pilot to quickly reverse the direction of an aircraft normal acceleration at specified accurate times, which is inherent to optimal maneuvers) and, therefore, may be employed as a kind of approximation of it. Whether the optimal maneuver converges to the vertical-S or the horizontal-S maneuvers depends on the employed nominal controls. Inasmuch as the missile acceleration command constraints Eqs. (8) and (9) give a square shape missile load factor ability envelope, that is, in the vertical (0 or 180 deg) or the horizontal ($\pm$90 deg) directions the missile can produce minimum lateral acceleration and the maximum in the skewed ($\pm$45 or $\pm$135 deg) directions, therefore, it is reasonable for the aircraft to evade in vertical or horizontal directions. Figure 10 shows MD in relation to barrel roll rate with the time to go of 3 s, where $\psi_{t0} = 165$ deg. The maximum value of MD is 20 m, which occurs at $\omega = 1.9$ rad/s.

Corresponding to the horizontal-S maneuver in Fig. 8, where the aircraft first takes a leftward acceleration and then reverses direction, another locally optimal maneuver exists, where the aircraft first takes a rightward acceleration and then reverses direction. Let us call this the a type and the former the b type. Figure 11 shows the MDs in relation to the initiation time of these two horizontal-S type maneuvers. The result shows that MD by the split-S or horizontal-S maneuvers (Figs. 8 and 11) is sensitive to time-to-go (maneuver initiation time) and, by the split-S, the maximum value of 10 m is produced at about 1 s time-to-go, whereas the HGB with $\omega = 2$ rad/s produces the maximum value of 20 m with more than 3 s time to go. Figure 11 also suggests which type of the horizontal-S maneuver produces larger MD in relation to the missile–aircraft initial geometry. In summary, the optimal evasive pattern obtained by

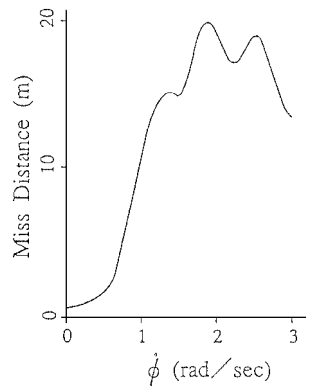

Fig. 10 MD by the HGB maneuver in relation to barrel roll rate (duration of maneuver 3 s).

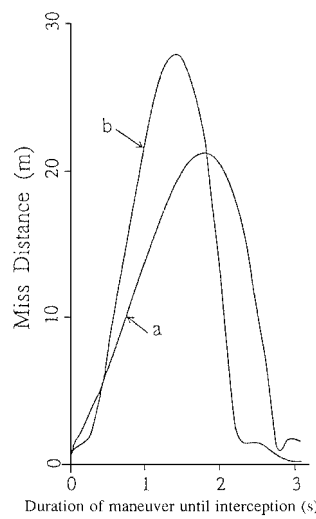

Fig. 11 MD in relation to duration of maneuver by two kinds of horizontal-S maneuvers.

numerical calculation shows the feature of the vertical-S type or the horizontal-S type, which produces about 27 m MD. However, inasmuch as it is difficult to implement these types of maneuvers accurately, the HGB may be employed as a practical approximation instead of them. Another point is that the result is obtained against the roll-stabilized missile. Therefore, there is a possibility that the HGB is optimal maneuver against a nonroll-stabilized missile, the study of which is beyond the scope of this paper.

IV. Conclusions

Two-dimensional and three-dimensional optimal evasive maneuvers of a fighter against a proportional navigation missile are obtained by numerical calculations, and their features are discussed in relation to HGB maneuvers. Even in the three-dimensional calculation, the optimal solutions converges to the two-dimensional evasive pattern that shows the feature of the vertical-S or the horizontal-S maneuver and produces about 27-m MD, but the value is very sensitive to time to go. On the other hand, the HGB with its roll rate about 2 rad/s produces MD of 20 m with more than 3 s time to go. As it is difficult for a pilot to implement optimal maneuvers accurately, the HGB may be employed as a practical approximation instead of them.

Appendix: Steepest Ascent Algorithm

A steepest ascent method, developed by Bryson and Denham,[8] is a well-known algorithm to solve nonlinear optimal control problems. A summary of the algorithm is shown here for the readers' convenience. For more detail, please refer to Refs. 8 and 9.

Find $\boldsymbol{u}(t)$ to maximize

$$J = \phi[\boldsymbol{x}(t_f)] \tag{A1}$$

where

$$\dot{\boldsymbol{x}} = \boldsymbol{f}(\boldsymbol{x}, \boldsymbol{u}, t) \tag{A2}$$

$$\boldsymbol{x}(t_0) = \bar{\boldsymbol{x}}_0 : \text{specified} \tag{A3}$$

with terminal constraints

$$\psi[\boldsymbol{x}(t_f), t_f] = 0 \tag{A4}$$

where $\boldsymbol{x}(t)$ is an n-dimensional state vector, $\boldsymbol{u}(t)$ is an m-dimensional control vector, and ψ is a q-dimensional constraint vector.

The terminal time t_f is determined from the following stopping condition:

$$\Omega[\bar{\boldsymbol{x}}(t_f), t_f] = 0 \tag{A5}$$

The optimal control $\bar{\boldsymbol{u}}(t)$ is obtained by the following algorithm:

1) Estimate a set of control variable histories $\bar{\boldsymbol{u}}(t)$ (which is called a nominal control).

2) Integrate the system equations (A2) with the initial condition (A3) and control variable histories from step 1 until Eq. (A5) is satisfied. Record $\boldsymbol{x}(t)$, $\boldsymbol{u}(t)$, and $\psi[\boldsymbol{x}(t_f)]$. Calculate the time histories of the $(n \times m)$ matrix of functions

$$G(t) = \frac{\partial \boldsymbol{f}}{\partial \boldsymbol{u}} \tag{A6}$$

3) Determine n-vector influence functions $\boldsymbol{\lambda}_\phi(t)$ and $\boldsymbol{\lambda}_\Omega(t)$ and $(n \times q)$ matrix of influence functions $\lambda_\psi(t)$, by backward integration of the following influence equations, using $\boldsymbol{x}(t_f)$ obtained in step 2 to determine the boundary conditions:

$$\dot{\boldsymbol{\lambda}}_\phi^T = -\boldsymbol{\lambda}_\phi \frac{\partial \boldsymbol{f}}{\partial \boldsymbol{x}} \tag{A7}$$

$$\dot{\boldsymbol{\lambda}}_\phi^T(t_f) = \left(\frac{\partial \phi}{\partial \boldsymbol{x}}\right)_{t_f} \tag{A8}$$

$$\dot{\boldsymbol{\lambda}}_\Omega^T = -\boldsymbol{\lambda}_\Omega \frac{\partial \boldsymbol{f}}{\partial \boldsymbol{x}} \tag{A9}$$

$$\boldsymbol{\lambda}_\Omega^T(t_f) = \left(\frac{\partial \Omega}{\partial \boldsymbol{x}}\right)_{t_f} \tag{A10}$$

$$\dot{\lambda}_\psi^T = -\lambda_\psi^T \frac{\partial \boldsymbol{f}}{\partial \boldsymbol{x}} \tag{A11}$$

$$\lambda_\psi^T(t_f) = \left(\frac{\partial \psi}{\partial \boldsymbol{x}}\right)_{t_f} \tag{A12}$$

Calculate the following influence functions $\boldsymbol{\lambda}_{\phi\Omega}(t)$ and $\lambda_{\psi\Omega}(t)$:

$$\boldsymbol{\lambda}_{\phi\Omega} = \boldsymbol{\lambda}_\phi - \frac{\dot{\phi}(t_f)}{\dot{\Omega}(t_f)} \boldsymbol{\lambda}_\Omega \tag{A13}$$

$$\lambda_{\psi\Omega} = \lambda_\psi - \frac{\dot{\psi}(t_f)}{\dot{\Omega}(t_f)} \lambda_\psi \tag{A14}$$

4) Simultaneously with step 3, compute the following integrals:

$$I_{\psi\psi} = \int_{t0}^{t_f} \lambda_{\psi\Omega}^T G W^{-1} G^T \lambda_{\psi\Omega} \, dt \tag{A15}$$

$$\bar{\boldsymbol{I}}_{\psi\phi} = \int_{t0}^{t_f} \lambda_{\psi\Omega}^T G W^{-1} G^T \boldsymbol{\lambda}_{\phi\Omega} \, dt \tag{A16}$$

$$I_{\phi\phi} = \int_{t0}^{t_f} \boldsymbol{\lambda}_{\phi\Omega}^T G W^{-1} G^T \boldsymbol{\lambda}_{\phi\Omega} \, dt \tag{A17}$$

5) Choose values of $\delta\psi$ to cause the next solution to be closer to the desired values $\psi[\boldsymbol{x}(t_f)] = 0$. For example, one might choose

$$\delta\psi = -\varepsilon\psi[\boldsymbol{x}(t_f)], \qquad 0 < \varepsilon \leq 1 \tag{A18}$$

The proper choice of $\delta\boldsymbol{u}(t)$, which increases J, is given as follows:

$$\delta\boldsymbol{u}(t) = (1/2\mu) W^{-1} G^T (\boldsymbol{\lambda}_{\phi\Omega} - \lambda_{\psi\Omega} \bar{\boldsymbol{\nu}}) \tag{A19}$$

where

$$2\mu = \left[\frac{I_{\phi\phi} - \boldsymbol{I}_{\psi\phi}^T I_{\psi\psi}^{-1} \boldsymbol{I}_{\psi\phi}}{(dp)^2 - d\psi^T I_{\psi\psi}^{-1} d\psi}\right]^{\frac{1}{2}} \tag{A20}$$

$$\bar{\boldsymbol{\nu}} = -2\mu I_{\psi\psi}^{-1} d\psi + I_{\psi\psi}^{-1} \boldsymbol{I}_{\psi\phi} \tag{A21}$$

where dp and $(m \times m)$ matrix of weighting functions $W(t)$ are chosen to satisfy

$$(dp)^2 = \int_{t0}^{t_f} \delta\boldsymbol{u}^T(t) W(t) \delta\boldsymbol{u}(t) \, dt \tag{A22}$$

6) Repeat steps 1–5, using an improved estimate of $\boldsymbol{u}(t)$ where

$$\boldsymbol{u}(t) = \boldsymbol{u}(t)_{\text{old}} + \delta\boldsymbol{u}(t) \tag{A23}$$

The key technique of the algorithm is the proper choice of the value dp, which must be changed every step, to avoid dropping into local optima, and to reach to the global optimum.

In our problem, variables are choosed as

$$\bar{\boldsymbol{x}} = (\gamma_t \quad \psi_t \quad \gamma_m \quad \psi_{\boldsymbol{m}} \quad r_x \quad r_y \quad r_z \quad a_p \quad a_y \quad p_m \quad p_t)^T \tag{A24}$$

where p_m and p_t are introduced to satisfy Eqs. (10), (11), and (19)

$$\dot{p}_m = \delta_m(a_{pc})(a_{pc} - a_{c\max})^2 + \delta_m(a_{yc})(a_{yc} - a_{c\max})^2 \quad \text{(A25)}$$

where

$$\delta_m(a) = 0 \qquad \text{for} \qquad |a| \le a_{c\max}$$
$$= 1.0 \qquad \text{for} \qquad |a| > a_{c\max}$$

$$\dot{p}_t = \delta_t(a_t)(a_{t\max} - a_t)^2 \quad \text{(A26)}$$

where

$$\delta_t(a) = 0 \qquad \text{for} \qquad |a| \le a_{t\max}$$
$$= 1.0 \qquad \text{for} \qquad |a| > a_{t\max} \quad \text{(A27)}$$

$$\psi = [p_m(t_f)\, p_t(t_f)]^T \quad \text{(A28)}$$

$$\Omega[\bar{x}(t_f)] = r_x\dot{r}_x + r_y\dot{r}_y + r_z\dot{r}_z \quad \text{(A29)}$$

where $\dot{r}_x$, $\dot{r}_y$, and $\dot{r}_z$ are given in Eqs. (4–6).

The initial estimates of control variables $\boldsymbol{u} = [a_t(t)\phi(t)]$ are

$$a_t(t) = a_{t\max} \quad \text{(A30)}$$

$$\phi(t) = \omega t + \phi_0 \quad \text{(A31)}$$

where ω is the HGB roll rate in Fig. 5; the value is changed from 1.0 to 2.0 and ϕ_0 is changed from 0 to π.

References

[1]Shinar, J., Rotszstein, Y., and Bezner, E., "Analysis of Three-Dimensional Optimal Evasion with Linearized Kinematics," *Journal of Guidance and Control*, Vol. 1, No. 5, 1979, pp. 353–360.

[2]Forte, I., Steinberg, A., and Shinar, J., "The Effects of Non-Linear Kinematics in Optimal Evasion," *Optimal Control Applications and Methods*, Vol. 4, 1983, pp. 139–152.

[3]Imado, F., and Miwa, S., "Fighter Evasive Maneuvers Against Proportional Navigation Missile," *Journal of Aircraft*, Vol. 23, No. 11, 1986, pp. 825–830.

[4]Zarchan, P., "Representation of Realistic Evasive Maneuvers by the Use of Shaping Filters," *Journal of Guidance and Control*, Vol. 2, No. 4, 1979, pp. 290–295.

[5]Gunston, B., and Spick, M., *Modern Air Combat*, Salamander Books, London, 1983, p. 202.

[6]Imado, F., and Miwa, S., "Three-Dimensional Study of Evasive Maneuvers of a Fighter Against Missile," AIAA Paper 86-2083, Aug. 1986.

[7]Imado, F., and Miwa, S., "Missile Guidance Algorithm Against High-g Barrel Roll Maneuvers," *Journal of Guidance, Control, and Dynamics*, Vol. 17, No. 1, 1994, pp. 123–128.

[8]Bryson, A. E., Jr., and Denham, W. F., "A Steepest Ascent Method for Solving Optimum Programing Problems," *Journal of Applied Mechanics*, Vol. 29, June 1962, pp. 247–257.

[9]Bryson, A. E., Jr., and Ho, Y. C., *Applied Optimal Control*, Ginn–Blaisdell, Waltham, MA, 1975, pp. 221–228.